IHJPAS. 36 (4) 2023

Ibn Al-Haitham Journal for Pure and Applied Sciences
Journal homepage: jih.uobaghdad.edu.iq

Monitoring Pollution and the Trend of Air Quality in Brick Factories in the Nahrawan Region and its Impact on Baghdad, Using Remote Sensing Data

Asmaa Mouhmmed Jadem*
Department of Biology, College of Sciences for Women, University of Baghdad, Baghdad, Iraq.

Israa Mohsin Jasem
Department of Biology, College of Sciences for Women, University of Baghdad, Baghdad, Iraq.

Fouad K. Mashee Al-Ramahi
Remote Sensing Unit, College of Sciences, University of Baghdad, Baghdad, Iraq.

***Corresponding Author: neranecology@uomisan.edu.iq**

Article history: Received 27 December 2022 Accepted 7 February 2023, Published in October 2023.

doi.org/10.30526/36.4.3162

Abstract

One of the most significant environmental issues facing the planet today is air pollution. Due to developments in industry and population density, air pollution has lately gotten worse. Like many developing nations, Iraq suffers from air pollution, particularly in urban areas with heavy industry. Our research was carried out in Baghdad's Al-Nahrawan neighbourhood. Recently, ground surveys and remote sensing were used to study the monitoring of air pollution. In order to extract different gaseous and particle data, the Earth Data Source, Google Earth Engine (GEE), and Geographic Information Systems (GIS) software were all employed. The findings demonstrated that there is a significant positive connection between data collected by ground-based devices and remote sensing platforms. The brick manufacturers' operations in the region's northwest and west directions from Baghdad were plainly having an impact on the region of Al-Air Nahrawan's quality. As a result, residents in the area are more likely to contract illnesses caused by pollution.

Keywords: Air Quality, Remote Sensing Data, Geographic Information System GIS, Google Earth Engine, Brick factories, Al-Nahrawan Region.

1. Introduction

One of the biggest environmental issues, which mostly affects cities, is air pollution. According to the WHO, air pollution is the contamination of an indoor or outdoor environment by chemical, physical, or biological factors that results in changes to the ambient air's normal characteristics and is detrimental to human health as well as the health of other living things [1]. With the advancement of industrialization and urbanization, air pollution in Asian cities has increased [2].

Mobility practices, waste management, the burning of fossil fuels such as coal, natural gas, and oil, industrial development (the brick and cement industries), the production and use of energy (for processing, heating, and cooking), the combustion of plastic and organic compounds, the incomplete combustion of synthetic materials, motor vehicles, and activities that produce dust and suspended particles are all examples of anthropogenic sources of air pollution in urban areas. Urban air pollution has a negative impact on public health that is seen globally [3].

Nitrogen oxides (NOx), carbon dioxides (COx), Sulphur dioxide (SO2), and particulate matter (PM), which is ambient solid particles, including several heavy metal ions such as vanadium and lead from gasoline additives, are among the harmful chemical compounds released to the atmosphere [4].

Ground surveys or in-situ measurements are commonly used to monitor air quality and identify atmospheric pollution. However [5], remote sensing has been widely employed in environmental applications, such as studies of air and water quality and geographic information systems (GIS), where the area and level impacted by air pollution may be shown more accurately and objectively. [6] [7].

By employing sensors mounted on a platform far from the earth's surface, remote sensing is a method for gathering data about the planet without physically touching or sampling it [7]. It offers frequently updated information on land-cover and land-use so users may monitor the density of water bodies, vegetation, towns, roads, open space, demographic information, and other elements [8] [9]. GIS technology allows locating the pollutants source and monitor the areas for change to conserve the quality of air, providing boundary condition to the air quality models [10] [11] [12]. In general, GIS models trends and spatial variations using remote sensing data as a database and various analyses, mapping, modelling, and visualization techniques [13] [14; 15].

The foci of this research are to identify air pollutants, gaseous components, and atmospheric particles (PM2.5, CO_2, CO, NO_2, SO_2, CH_4, and O_3) along Al-Nahrawan region in Baghdad and examine their relationship with meteorological parameters such as temperature, relative humidity, and precipitation to determine their impact in 2022 using satellite data. The study also examines the influence of the nearby brick manufacturers on the region's biodiversity and how air pollution is distributed in the area [1].

2.Material and Methods

2.1.Description of Region of Study

The study area is Al-Nahrawan city located in the southeast direction of Baghdad. Baghdad is the capital city of Iraq, lying between longitude 33.35° N and latitude 44.45° E**. Figure 1** depicts a map of the research region. There are more than 266 brick industries there; the largest brick factory complex in Baghdad is a leather tanning complex, and 66 laboratories are really operated by the more than 266 brick manufacturers because of the poor working conditions and expensive worker pay.

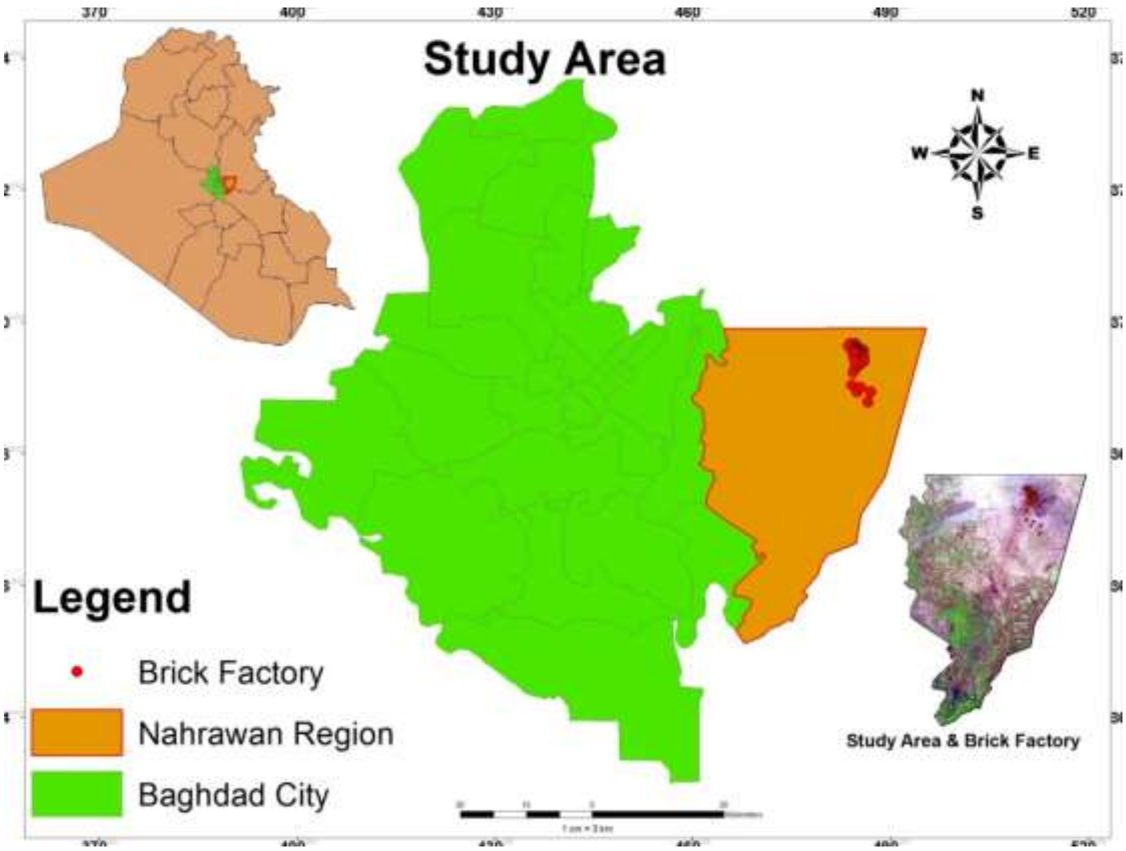

Figure 1. Map showing the study area of Al-Nahrawan region (area) and the brick factories inside it.

2.2.Data Acquisition

2.2.1.Ground Base measurements

The sampling was carried out during July 2022, with 10 sampling points distributed in the Al-Nahrawan region, as shown in Table 1.

Table 1. The X Y coordination.

Samples	X-axis coordinate	Y-axis coordinate
1	44.50269	33.22559
2	44.50566	33.22552
3	44.50436	33.22579
4	44.50082	33.23091
5	44.50454	33.23116
6	44.50333	33.23107
7	44.50031	33.23248
8	44.43288	33.22212
9	44.42287	33.22212
10	44.40439	33.22175

2.2.2.Satellite Measurements

In the current investigation, ground measurements of pollutant concentrations were taken using a Gas Met device at ten distinct sites in Al-Nahrawan suburban. These data were used to determine the accuracy of the satellite observations. The Google Earth Engine (GEE) platform was used to extract the meteorological parameters (Temperature, Specific humidity, Precipitation) as well as the gaseous concentrations (Particulate Matters PM 2.5, Carbon Monoxide, Nitrogen Dioxide, Ozone, Sulphur Dioxide, and Methane). Carbon Dioxide concentration was obtained from Earth Data. After obtaining the spatial data of the average seasonal air pollution chemicals from GEE, the ARCGIS application was used to create the maps showing the distribution of air pollutants [15].

Satellite images from passive sensors were analysed for this study. In order to monitor land cover, meteorological, and air pollutant parameters, a variety of spatial and temporal data types and sources are gathered using the instruments listed in Table 1.

Table 2. Description of imagery datasets.

Sensor	Extracted Data
Global Forecast System (GFS)	Maximum, Minimum, Average (Mean) on daily bases of temperature
Global Forecast System (GFS)	Maximum, Minimum, Average (Mean) on daily bases of relative humidity
Climate Hazards group Infrared Precipitation with Stations (CHIRPS)	Precipitation daily bases
Copernicus Atmosphere Monitoring Service (CAMS)	PM2.5 daily average bases
Sentinel-5P	pollutants measurements of NO_2, SO_2, O_3, CH_4, CO
Orbiting Carbon Observatory (OCO_2) satellite	CO_2 concentration
Normalized Difference Vegetation Index NDVI	quantity of actively photosynthesizing biomass

3.Results and Discussion

3.1.*In situ* Ground Base Measurements

The air pollutant sampling was carried out for a day in July 2022 according to the 10 ground points by ground device measurement as shown in **Table 3**.

Table 3. Concentrations of air polluting gases and particles and statistic result from ground device during July 2022.

	Ground Measured Data										**Statistical Result**		
Sample	**1**	**2**	**3**	**4**	**5**	**6**	**7**	**8**	**9**	**10**	**Max**	**Min**	**Average**
CO_2 (ppm)	553	555	583	479	478	516	476	475	504	509	583	474	512
CO (molecules cm^{-2})	0.55	0.9	0.26	0	0.1	2.63	0.61	0.1	0.47	0.14	2.63	0	0.576
N_2O (molecules cm^{-2})	0.3	0.31	0.29	0.29	0.31	0.32	0.29	0.32	0.33	0.34	0.34	0.29	0.31
CH_4 (ppb)	1.95	2.05	2.12	1.97	1.89	2.32	1.98	2.03	2.01	2.06	2.32	1.89	2.038
NO_2 (molecules cm^{-2})	0.27	0.28	0.48	0.37	0.35	0.06	0.1	0	0.07	0.15	0.48	0	0.213
SO_2 (molecules cm^{-2})	0.18	0	0	0	0	0	0	0	0.73	0	0.73	0	0.091
T (^{0}C)	30	32	33	33	34	35	36	37	37	38	38	30	34.5

3.2.Satellite Measurement results

The air pollutant data shown in **Table 4** was extracted from GEE for the same day in July 2022 from the same 10 points distributed in the Al-Nahrawan region (see Table 1). The wind is blowing in a southwest direction..

Table 4. Concentrations of air polluting gases and statistic result from Satellite during July 2022**.**

	Sample	**CO (molecules cm^{-2})**	**CO_2 (ppm)**	**NO_2 (molecules cm^{-2})**	**SO_2 (molecules cm^{-2})**	**CH_4 (ppb)**
Satellite Measured Data	**1**	2.91E+18	536	1.40E+16	1.56E+13	1925
	2	2.91E+18	542	1.50E+16	1.22E+13	1925
	3	2.11E+18	560	1.29E+16	1.22E+13	1925
	4	2.11E+18	510	1.29E+16	1.22E+13	1925
	5	2.11E+18	488	1.49E+16	1.22E+13	1925
	6	2.90E+18	480	1.29E+16	1.22E+13	1970
	7	2.80E+18	452	1.18E+15	1.22E+13	1925
	8	2.11E+18	478	1.50E+15	1.22E+13	1925
	9	2.11E+18	512	1.50E+15	2.96E+13	1925
	10	2.11E+18	519	1.83E+15	2.16E+13	1925
Statistical Result	**Max**	2.91E+18	560	1.50E+16	2.96E+13	1970
	Min	2.11E+18	452	1.18E+15	1.22E+13	1925
	Average	2.42E+18	507.7	8.85E+15	1.52E+13	1.93E+03

3.3.Comparison of satellite data and analysis of ground samples

The satellite-based data products derived using Google Earth Engine GEE must be statistically correlated with the majority of the independent ground-based datasets in order to ensure the validity of the satellite findings [16].

A study conducted in the Al-Nahrawan region found that the brick and tanning companies that make up the industrial process are the primary causes of the region's high pollution levels. In July 2022, the relationship between the satellite and ground device measurements from ten sites was similar for the pollutants CO, CO_2, NO_2, SO_2, CH_4 in July 2022. However, the R^2 of the relation between the measurements of the satellite and ground device of CO pollutant was 0.46 (**Figure 2-A**), CO_2 was 0.72 **(Figure 2-B)**, SO_2 was 0.74 (**Figure 2-C**), NO_2 was 0.55 (**Figure 2-D**), and CH_4 was 0.7 (**Figure 2-E**) in July 2022.

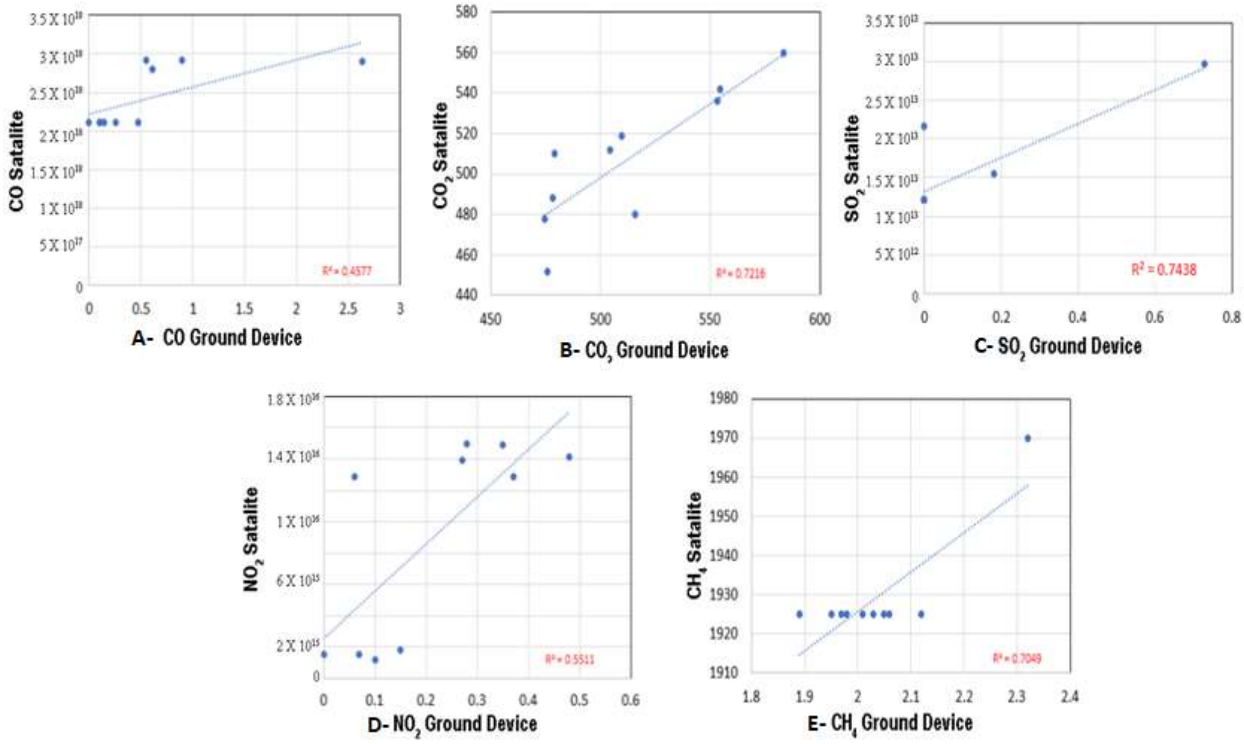

Figure 2. Data relation between satellite-based tropospheric column number density and ground-based measurements of different gases.

Table 5 shows the Pearson correlation between both variables of satellite-based and ground-based observations. The highest correlation was for SO_2 at 0.86 (p-value < 0.05), followed by CO_2, CH_4 and NO_2 at 0.85 (p-value < 0.05), 0.84 (p-value < 0.05), and 0.72 (p-value < 0.05), respectively. The least one was for CO of 0.68 (p-value < 0.05). All correlations were greater than 0.5. This means that there is a strong positive correlation between ground and satellite readings. Thus, the extracted data are verified [17].

Table 5. Person correlation statistics results for different locations in the Al-Nahrawan region at July 2022 between both variables of satellite-based and ground-based observations.

Air pollutants	Pearson Correlation Coefficient	Correlation significant level (p-value)
NO_2	0.72	< 0.05
SO_2	0.86	< 0.05
CH_4	0.84	< 0.05
CO_2	0.85	< 0.05
CO	0.68	< 0.05

3.4.Relation between Air Pollutants Components.

It is possible to determine whether or not temperature, precipitation, and relative humidity have an impact on the quantity of air pollutants in the Al-Nahrawan region by analysing these variables. The primary sources of pollution in Al-Nahrawan are brick manufacturers and the western side of Baghdad.

In Iraq's brick industry, for instance, there are still antiquated combustion methods in use, and no treatment facilities are present. The toxic substances that seep from these brick kilns adversely affect the soil, nearby plants, nearby people, and nearby animals, with brick workers, women, and children suffering the worst effects [18].

Figure 3-A shows that the relationship between relative humidity and temperature is linear and normal, with an R2 value of 0.84 and a significant negative Pearson correlation of 0.91 and a p-value of 0.05.

According to **Figure 3-B**, relative humidity and precipitation have a positively significant Pearson correlation (r = 0.82, p-value 0.05) and are linearly associated in a normal relationship with each other.

According to **Figure 3-C**, precipitation and temperature have a significant negative Pearson correlation (r= -0.74, p-value= 0.05) and a linear correlation in a normal relationship with a value of R2=0.57.

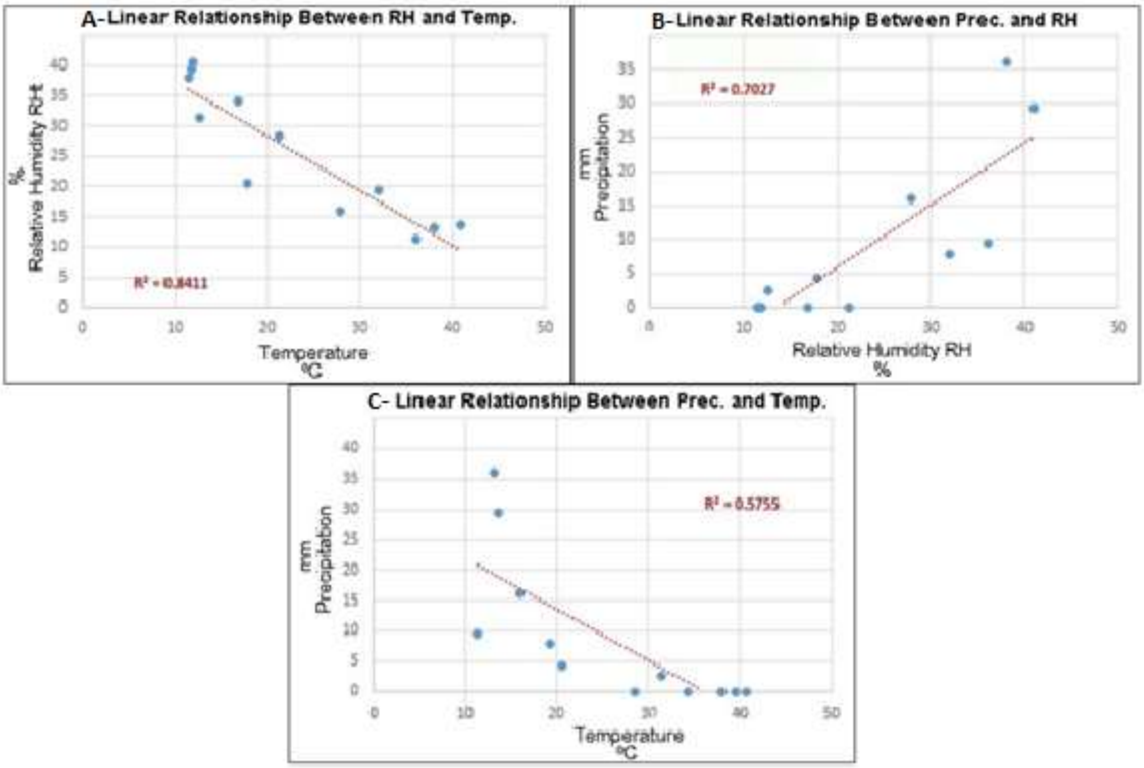

Figure 3. Linear relationship between precipitation, temperature, and relative humidity.

As demonstrated in **Figure 4-A**, sulfur dioxide SO2 and temperature exhibit a strong linear association with a value of R2=0.5 and a strong negative significant Pearson correlation (r=-0.71, p-value= 0.01).

As indicated in **Figure 4-B**, methane CH4 and precipitation were linearly interrelated in a normal relationship with a value of R2=0.42 and a strong negative significant Pearson correlation (r=-0.65, p-value=0.02).

As demonstrated in **Figure 4-C**, methane CH4 and temperature are linearly associated in a normal relationship with a value of R2=0.25 and a strong positive Pearson correlation (r= 0.5, p-value= 0.09).

As shown in **Figure 4-D**, carbon dioxide CO_2 and precipitation were linearly correlated in a normal relationship with a value of R^2=0.25, and they had a significant negative Pearson correlation (r=-0.5, p-value=0.09). The intensive fuel burning required for the production of bricks is the cause of the high increase in CO_2 concentration. Additionally, the lack of vegetation in the Al-Nahrawan study area contributes to the rising CO_2 levels.

According to **Figure 4-E**, precipitation and sulfur dioxide SO_2 have a high positive significant Pearson correlation (r= 0.66, p-value= 0.02) and a linearly high correlation with a value of R2=0.43.

According to **Figure 4-F**, relative humidity and sulfur dioxide SO_2 have a high positive significant Pearson correlation (r= 0.82, p-value= 0.01) and a linearly correlated relationship with a value of R^2=0.67.

Table 6. Pearson correlation between the atmospheric substances over Al-Nahrawan region**.**

	Temperature ^{0}C	**Precipitation mm**	**Relative Humidity %**	**CO**	**CO_2**	**$PM_{2.5}$**	**NO_2**	**SO_2**
Temperature ^{0}C	1	-0.73	-0.91	-0.23	0.2	-0.07	0.14	-0.7
Precipitation	-0.73	1	0.82	0.03	-0.51	-0.03	-0.12	0.64
Relative Humidity %	-0.91	0.82	1	0.07	-0.21	-0.15	0.06	0.82
CO	-0.23	0.03	0.07	1	-0.54	0.22	0.41	0.12
CO_2	0.2	-0.51	-0.21	-0.54	1	-0.26	-0.05	-0.07
$PM_{2.5}$	-0.07	-0.03	-0.15	0.22	-0.26	1	-0.16	-0.08
NO_2	0.14	-0.12	0.06	0.41	-0.05	-0.16	1	0.45
SO_2	-0.7	0.64	0.82	0.12	-0.07	-0.08	0.45	1
CH_4	0.49	-0.67	-0.33	-0.13	0.49	-0.55	0.46	-0.23

Table 7. P-value for Pearson correlation between the atmospheric substances over Al-Nahrawan region.

	Temperature ^{0}C	**Precipitation mm**	**Relative Humidity %**	**CO**	**CO_2**	**$PM_{2.5}$**	**NO_2**	**SO_2**
Temperature ^{0}C	0	0.007	0	0.476	0.529	0.836	0.661	0.011
Precipitation	0.007	0	0.001	0.915	0.092	0.934	0.701	0.026
Relative Humidity %	0	0.001	0	0.825	0.517	0.638	0.856	0.001
CO	0.476	0.915	0.825	0	0.073	0.484	0.186	0.722
CO_2	0.529	0.092	0.517	0.073	0	0.418	0.887	0.825
$PM_{2.5}$	0.836	0.934	0.638	0.484	0.418	0	0.612	0.797
NO_2	0.661	0.701	0.856	0.186	0.887	0.612	0	0.142
SO_2	0.011	0.026	0.001	0.722	0.825	0.797	0.142	0
CH_4	0.105	0.017	0.288	0.689	0.105	0.064	0.133	0.481

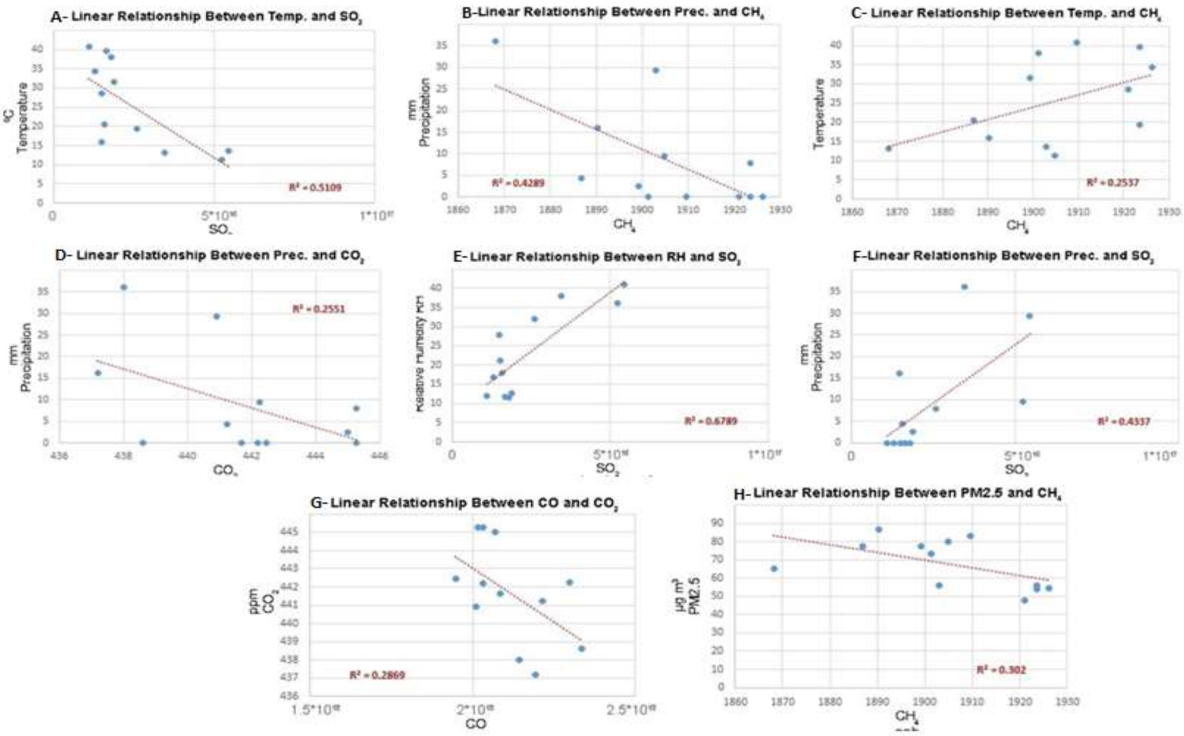

Figure 4. The Linear relationship between air substances.

The brick factories' industrial activity, which uses a lot of fuel oil to finish the brick-making process, is what causes the CO. The incomplete combustion of fuel produces CO, which causes an increase in its concentration in the Al-Nahrawan study area.

As shown in **Figure 4-G**, CO and CO_2 have a linear correlation in a normal relationship with each other with a value of R^2=0.28. They also have a significant negative Pearson correlation (r=-0.54, p-value=0.073).

As shown in **Figure 4-H**, PM2.5 and Methane CH_4 have a linear correlation in a normal relationship with a value of R^2=0.3 and a significant negative Pearson correlation (r=-0.55, p-value=0.06).

According to the results of the NO_2, SO_2, CH_4, and CO pollution distribution, brick firms produce a substantial amount of pollutants in the Al-Nahrawan region. Furthermore, as settlements are to blame for indoor pollution, it is assumed that pollution is worse in densely inhabited locations. It is likely that their shared source is to blame when pollutants are proven to positively correlate with one another across various regions. To evaluate if and how strongly two variables are associated, one might use a statistical technique called correlation [19].

The displayed normalized difference vegetation index (NDVI) represents the vegetation cover in the Al-Nahrawan region. The maximum, however, was (0.3) in February and March, when precipitation was at its highest and temperatures were at their lowest. With an R^2 value of 0.48 and a strong positive and significant Pearson correlation (r= 0.7, p-value= 0.05), NDVI and precipitation have a linearly connected relationship. While the NDVI and temperature have a strong linear link with an R^2 of 0.6, they also have a strong negative significant Pearson correlation (r = -0.8, p-value = 0.05). Additionally, the NDVI and temperature show a strong linear link with an R^2 of 0.38 and a high positive and significant Pearson correlation (r=0.62, p-value=0.05) **Figure 5**.

The NDVI was correlated with CO_2 and CH_4, NDVI and CH_4 exhibit a strong linear association with an R^2 of 0.6 and a strong negative significant Pearson correlation (r= -0.77, p-value 0.05), respectively. This suggests that the presence of vegetation may contribute to a reduction in the amount of methane present in the region [20; 16]. With a value of R2=0.4, NDVI and CO_2 have a strong linear relationship with one another. Additionally, they have a strong negative and significant Pearson correlation (r=-0.63, p-value = 0.05) **Figure 5**.

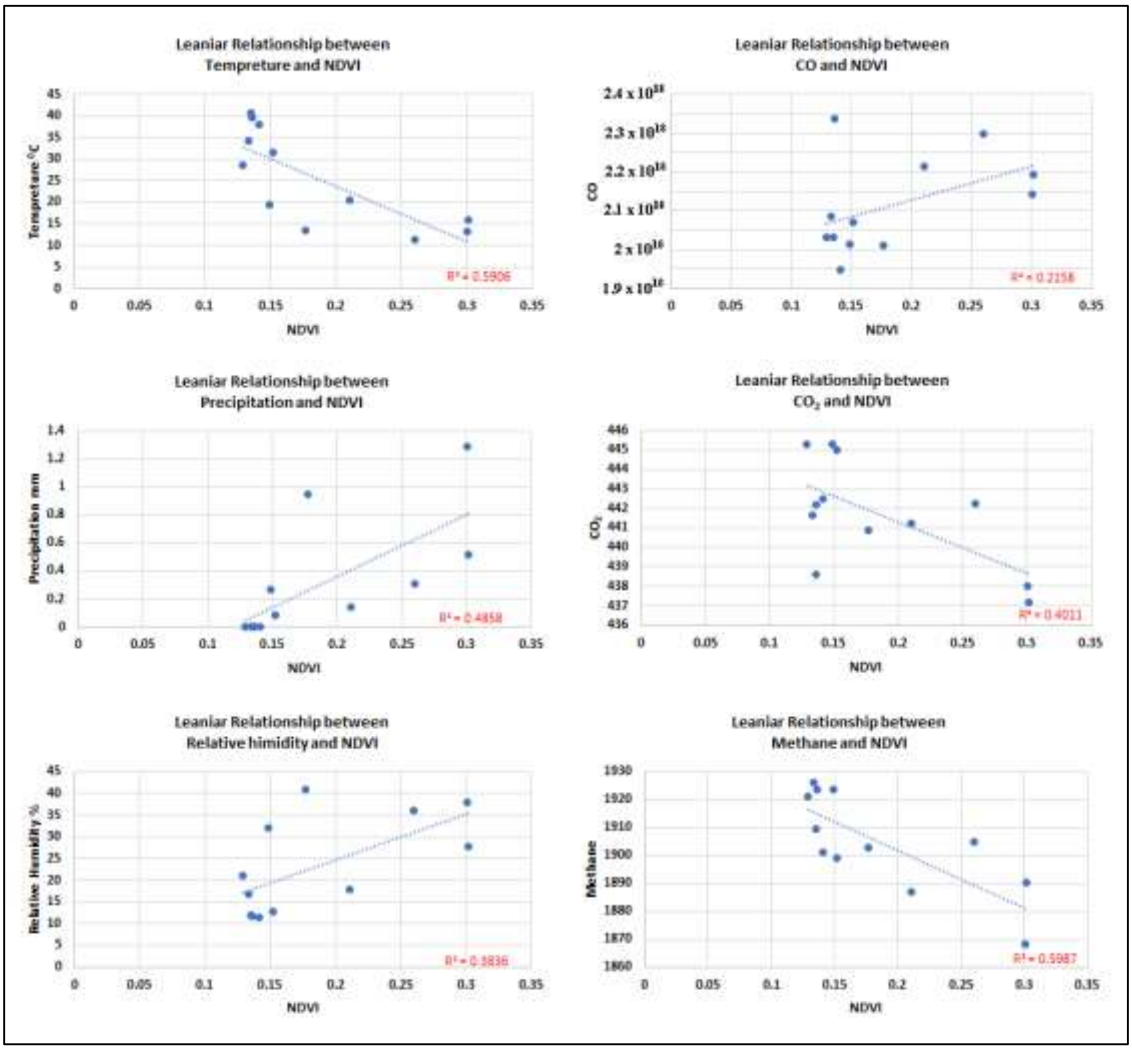

Figure 5. Linear relationship between NDVI and air substances.

4.Conclusion

The Al-Nahrawan Region is highly impacted by the pollutants released from brick factories in the region's northeast, and it was also discovered that Baghdad's emissions in the region's west also have a significant impact on the region. Limited data from the ground-based device can be analysed to enhance data collection methods, look into software capabilities, and validate data from the satellite.

In the fields of urban management and environmental studies, GIS and remote sensing have proven to be useful, intelligent, and productive technologies. By employing satellites, remote sensing assisted in estimating the level of pollution over the whole Al-Nahrawan region and provided a way to look into the source of the pollution. In the Al-Nahrawan region, brick factories have a significant impact on the water quality. Additionally, the use of indoor heating during the winter and fuel for transportation are additional sources of pollution and particulate matter in the Al-Nahrawan region. As a result, residents of the area are more likely to contract diseases caused by pollution.

References

1. Al-Alola, S.S.; Alkadi, I.I.; Alogayell, H.M.; Mohamed, S.A.; Ismail, I.Y. Air quality estimation using remote sensing and GIS-spatial technologies along Al-Shamal train pathway, Al-Qurayyat City in Saudi Arabia *Environ. Sustain. Indic*., **2022**; 15, 100184,
2. Al Naqeeb, N.A.; Al Hassany,J.S.; Mashee, F.K. Use Remote Sensing Techniques to Study Epiphytic Algae on Phragmites australis in Um El-Naaj Lake, Mysan Province, Southern Iraq. *IOP Conf. Ser. Earth Environ. Sci*., **2022**; 1002, 1.
3. Kang, B.; Liu, C.; Miao, C.; Zhang, T.; Li, Z.; Hou, C.; Li, H.; Li, C.; Zheng, Y.; Che, H. A Comprehensive Study of a Winter Haze Episode over the Area around Bohai Bay in Northeast China: Insights from Meteorological Elements Observations of Boundary Layer. *Sustainability*, **2022**, 14, 5424.
4. Rasheed, M.J.; Al-Ramahi, F.K.M. Detection of the impact of climate change on desertification and sand dunes formation east of the tigris river in salah al-din governorate using remote sensing techniques. *Iraqi Geol. J*., **2021**; *54*, 1, 69–83.
5. Al-Ramahi, F.K.M.; Shnain, A.A.; Ali, A.B. The Modern Techniques in Spatial Analysis to Isolate, Quarantine the Affected Areas and Prevent the Spread of COVID-19 Epidemic. *Iraqi J. Sci*., **2022**; *63*, 9, 4102–4117.
6. Chowdhury, S.; Al-Zahrani, M..; Abbas, A. Implications of climate change on crop water requirements in arid region: An example of Al-Jouf, Saudi Arabia. *Journal of King Saud University - Engineering Sciences*, **2016**; *28*, 1, 21–31.
7. Buckner C.A. We are IntechOpen, the world ' s leading publisher of Open Access books Built by scientists , for scientists TOP 1 %. *Intech*, **2016**; *11*, 13.
8. Dadvand, P.; Rushton, S.; Diggle, P.J.; Goffe, L.; Rankin, J.; Pless-Mulloli, T. Using spatio-temporal modeling to predict long-term exposure to black smoke at fine spatial and temporal scale. *Atmospheric Environment*, **2011**; *45*, 3, 659–664.
9. Weng, Q.; Yang, S. Urban Air Pollution Patterns, Land Use, and Thermal Landscape: An Examination of the Linkage Using GIS. *Environmental Monitoring and Assessment*, **2006**; *117*(1–3), 463–489.
10. Alias, M.; Hamzah, Z.; Kenn, L.S. Pm 10 and Total Suspended Particulates (Tsp) Measurements in Various Power Stations. *Malaysian J. Anal. Sci.*, **2007**; *11*, 255-261.
11. Zhang, Y.; Guindon, B. Using satellite remote sensing to survey transport-related urban sustainability. *International Journal of Applied Earth Observation and Geoinformation*, **2006**; *8*, 3, 149–164.
12. Mahal, S.H.; Al-Lami, A.M.; Mashee, F.K. Assessment of the Impact of Urbanization Growth on the Climate of Baghdad Province Using Remote Sensing Techniques. *Iraqi J. Agric. Sci.*, **2022**; *53*, 5, 1021–1034.

13. Sohrabinia, M.; Khorshiddoust, A.M. Application of satellite data and GIS in studying air pollutants in Tehran. *Habitat International*, **2007**; *31*, 2, 268–275.

14. Ahmed S.M.; Al-Ramahi, F.K.M.Evaluate the Effect of Relative Humidity in the Atmosphere of Baghdad City urban expansion Using Remote Sensing Data. *Iraqi J. Sci*., **2022**; *63*, 4, 1848–1859.

15. Mohammed Ali, A.K; Al Ramahi, F.K.M. A study of the effect of urbanization on annual evaporation rates in Baghdad city using remote sensing. *Iraqi J. Sci.*, **2020**; *61*, 8, 2142–2149.

16. Y Al Fahdawi, Y.M.N.; Al Ramahi, F.K.M.; Alfalahi, A.S.H. Measurement Albedo Coefficient for Land Cover (Lc) and Land Use (Lu), Using Remote Sensing Techniques, A Study Case: Fallujah City. *J. Phys. Conf. Ser*., **2021**; *1829*, 1.

17. FKhanjer, E.; AYosif, M.; ASultan, M. Air Quality Over Baghdad City Using Ground and Aircraft Measurements. *Iraqi Journal of Science*, **2015**; *56*.

18. Hussain, A.; Khan, N.; Ullah, M.; Imran, M.; Ibrahim, M.; Hussain, J.; Ullah, H.; Ullah, I.; Ahmad, I.; Khan, M.; Ali, M.; Attique, F. Brick Kilns Air Pollution and its Impact on the Peshawar City. *Pollution*, **2022**; *8*, 4, 1266-1273.

19. Freedman, D.S.; Mei, Z.; Srinivasan, S.R.; Berenson, G.S.; Dietz, W.H. Cardiovascular Risk Factors and Excess Adiposity Among Overweight Children and Adolescents: The Bogalusa Heart Study. *J. Pediatr*., **2007**; 150, 1, 12-17.e2.

20. Javadinejad, S.; Eslamian, S.; Ostad-Ali-Askari, K. Investigation of monthly and seasonal changes of methane gas with respect to climate change using satellite data. *Appl. Water Sci*., **2019**; *9*, 8, 1–8.